JMEPEG (2011) 20:306–316
DOI: 10.1007/s11665-010-9671-8

1059-9495/$19.00

Box-Behnken Design of Experiments Investigation of Hydroxyapatite Synthesis for Orthopedic Applications

S. Kehoe and J. Stokes

(Submitted February 6, 2009; in revised form March 5, 2010)

Physicochemical properties of hydroxyapatite (HAp) synthesized by the chemical precipitation method are heavily dependent on the chosen process parameters. A Box-Behnken three-level experimental design was therefore, chosen to determine the optimum set of process parameters and their effect on various HAp characteristics. These effects were quantified using design of experiments (DoE) to develop mathematical models using the Box-Behnken design, in terms of the chemical precipitation process parameters. Findings from this research show that the HAp possessing optimum powder characteristics for orthopedic application via a thermal spray technique can therefore be prepared using the following chemical precipitation process parameters: reaction temperature 60 °C, ripening time 48 h, and stirring speed 1500 rpm using high reagent concentrations. Ripening time and stirring speed significantly affected the final phase purity for the experimental conditions of the Box-Behnken design. An increase in both the ripening time (36-48 h) and stirring speed (1200-1500 rpm) was found to result in an increase of phase purity from 47(±2)% to 85(±2)%. Crystallinity, crystallite size, lattice parameters, and mean particle size were also optimized within the research to find desired settings to achieve results suitable for FDA regulations.

Keywords Box-Behnken, chemical precipitation, design of experiments, hydroxyapatite, optimization

1. Introduction

HAp and other related calcium phosphate minerals are used extensively to improve the integration of femoral implants in hip-joint therapy. HAp appears the most promising due to its outstanding biological properties such as atoxicity, lack of inflammatory response, and absence of fibrous or immunological reactions (Ref 1). HAp possesses identical chemical composition and high biocompatibility with that of natural bone (Ref 2). The bioactive nature of HAp gives rise to a favorable reactive product, through a chemical transformation of its starting material to the desired final implant. Subsequently, when HAp comes in contact with physiological fluids, a chemical reaction toward the production of newly formed bone takes place, in what is also termed as an osteoconductive process (Ref 1). Bioactivity is related to a modification of the surface of the material with formation of naturally induced, biologically equivalent HAp, as a result of dissolution, precipitation and ion exchange reactions with the physiological environment. This ability to bond to bone tissue without the formation of a fibrous tissue layer at the bone-implant interface is extremely important since it guarantees the fixation and stabilization of implants and prostheses (Ref 2-4). The bone-implant interface mimics the type of interface that is formed when natural tissues repair themselves; it is dynamic in its nature, changes with time and requires a controlled degree of chemical reactivity of the ceramic (Ref 1). Hence, the clinical advantage of HAp is its bioactive characteristics, which is dependent upon its synthetic structure (such as, chemical stoichiometry and crystallinity) (Ref 1). HAp has many crystallographic features that are similar to those of natural bone tissue; although they show insufficient mechanical reliability for medical applications where high loads are required (Ref 1).

Plasma thermal spray processes have frequently been used to deposit functionally biomedical active coatings, such as HAp, onto prosthetic implants (Ref 5, 6). Kweh et al. (Ref 2) confirmed from their investigations, that the quality of a HAp coating onto substrate is closely dependent on the overall attributes and characteristics of the synthesized powder.

In the literature, several methods used to prepare HAp crystals have been reported, including solid-state reactions, crystal growth under hydrothermal conditions, layer hydrolysis of other calcium phosphate salts, sol-gel crystallization, and precipitation methods (Ref 7). Variations in parameters that affect the synthesis are necessary in order to produce HAp of desired powder characteristics, such as: crystallinity, phase composition, particle size, and specific surface area (Ref 8, 9). Generally, wet methods produce greater amounts of HAp, are cost-effective and its only by-product is that of water. However, it is difficult to obtain HAp of stoichiometric composition. In this study, the chemical precipitation method was used to obtain pure, stoichiometric and crystalline HAp is based on the following reaction of orthophosphoric acid with calcium hydroxide:

$$10Ca(OH)_2 + 6H_3PO_4 \rightarrow Ca(PO_4)_6(OH)_2 + 18H_2O \quad \text{(Eq 1)}$$

Calcium-deficient HAp powder is a serious disadvantage, since nonstoichiometric HAp decomposes, during heat treatments, to more soluble solid phases. The aim of this work is to examine the influence of influential process variables on HAp physicochemical properties and determine an optimum set of process variables to produce HAp powder of desired

S. Kehoe and **J. Stokes**, MPRC, Materials Processing Research Centre and NCPST, National Centre for Plasma Science and Technology, Dublin City University, Dublin 9, Ireland. Contact e-mail: joseph.t.stokes@dcu.ie.

characteristics for optimum coating application using thermal spray application onto femoral implants, to satisfying regulatory requirements (Ref 10-13). Initially, a screening design of experiments (DoE) was conducted to identify the most influential parameters (as found from literature; Ref 3, 9, 14-18). The factors were investigated at two levels (+1(high) and −1(low)) and included, reaction synthesis temperature during precipitation, stirring speed, ripening time, acid addition rate, initial calcium concentration, and atmospheric environment (synthesis with and without a controlled atmospheric environment). These were evaluated against powder-related parameters such as: phase purity, crystallinity, crystallite size (L_{002} and L_{300}), lattice parameters, and particle size (Ref 19). This research only focuses on the factors which had and effect on the responses described above and within the ranges determined in the previous research (Ref 19) to fully optimize the HAp powder characteristics.

2. Materials and Methods

The optimization DoE experimental plan was based on the Box-Behnken experimental design, with three levels on the three most influential factors (determined from the screening analysis; Ref 19) were used to apply a full quadratic polynomial model, including interaction effects. Main and interaction effects were evaluated using the Design Expert 7.1 software (Stat-Ease) to investigate an optimized set of conditions for HAp synthesis using the chemical precipitation route. The Box-Behnken designs included two strategies (Ref 20): (i) centerpoints and (ii) points lying on one sphere, equally distant from the centerpoint. The latter points consist of small two-level full factorials where some factors are fixed at their center values. The number of centerpoints (five) was chosen to establish rotatability.

The three key controllable process factors (out of the following chosen in the screening design: reaction synthesis temperature during precipitation, stirring speed, ripening time, acid addition rate, initial calcium concentration, and atmospheric environment) were selected, based upon the evaluation of the significant main and interaction effects of the preliminary screening phase (Ref 19), comprised of T_o: reaction synthesis temperature (40, 50, and 60 °C), V_{st}: stirring speed (900, 1200, and 1500 rpm), and t_r: ripening time (24, 36, and 48 h). Each level representing minimum (−1), centerpoint (0), and maximum values (+1), respectively. Therefore 17 experimental runs were conducted. The processing region for the three process factor was limited to the region over which existing published literature had indicated as desirable values and was also selected based on the results as obtained at the preliminary screening stage of the DoE (Ref 19).

To optimize fully the responses ($Y_1 - Y_6$), an appropriate approximation for the true functional relationship between the independent variables and the response surface was identified, using the following second-order quadratic polynomial model for response surface method (RSM) design, as follows:

$$Y = b_0 + \sum b_i X_i + \sum b_{ij} X_i X_j + \sum b_{ii} X_{ii}^2 + \varepsilon, \qquad \text{(Eq 2)}$$

where i, j vary from 1 to the number of process variables, coefficient b_0 is the mean of responses of all the experiment, b_i coefficient represents the effect of the variable X_i, and b_{ij}, are the coefficients of regression which represent the effects of interactions of variables X_iX_j, and b_{ii}, are the coefficients of regression which represent the effects of interactions of the variable X_iX_i, and ε is the experimental error.

This model was used to evaluate the same responses ($Y_1 - Y_6$) as that evaluated in the screening stages of the design, such as Y_1 the phase purity, X_p (%), Y_2 the crystallinity, X_c (%), Y_3: crystallite size in the 002 plane, X_s, L_{002} (nm), Y_4 the crystallite size in the 300 plane, X_s, L_{300} (nm), Y_5 the a/c ratio, and Y_6 the particle size, P_s (μm). The responses were measured in sequential order for each experiment and performed in triplicate. The design matrix of experiments, in real values, obtained according to the optimized Box-Behnken design, as shown in Table 1. Centerpoint runs were interspersed among

Table 1 Box-Behnken experimental design and phase purity (X_p), crystallinity (X_c), crystallite size (X_s, L_{002}, and L_{300}), lattice parameter ratio (a/c), and mean particle size (P_s) of the different HAp samples for various conditions of synthesis temperature (T_o), stirring speed (V_{st}), and ripening time (t_r)

Sample	T_o, °C	V_{st}, rpm	t_r, h	Purity, X_p, %	Crystallinity, X_c, %	Crystallite size, X_s, L_{002}, nm	Crystallite size, X_s, L_{300}, nm	Lattice parameter, a, nm	Lattice parameter, c, nm	Mean particle size, P_s, μm
N1	40	900	36	72.24	75.12	57.42	58.29	9.4195	6.8934	28.04
N2	60	900	36	49.62	76.47	51.34	47.29	9.4484	6.8858	24.63
N3	40	1500	36	84.56	76.4	56.53	81.38	9.4058	6.8650	28.20
N4	60	1500	36	57.79	82.36	53.52	61.78	9.4246	6.8867	26.71
N5	40	1200	24	61.04	77.95	48.99	62.37	9.4279	6.8650	26.45
N6	60	1200	24	23.53	82.52	80.01	72.55	9.4720	6.8498	40.95
N7	40	1200	48	60.26	78.94	53.68	72.55	9.4282	6.8780	26.62
N8	60	1200	48	18.71	80.98	69.41	65.10	9.4312	6.8565	34.22
N9	50	900	24	50.50	72.81	66.00	56.00	9.4322	6.8558	37.07
N10	50	1500	24	71.16	79.18	59.19	69.65	9.4775	6.8525	27.99
N11	50	900	48	55.27	73.87	51.44	48.84	9.4245	6.8859	25.55
N12	50	1500	48	84.73	77.36	57.78	48.84	9.4456	6.8887	32.28
N13	50	1200	36	48.62	72.10	51.16	72.59	9.4186	6.8681	24.36
N14	50	1200	36	49.79	73.00	51.66	72.59	9.4186	6.8681	26.39
N15	50	1200	36	47.98	71.78	51.26	73.00	9.4186	6.8681	27.37
N16	50	1200	36	47.65	72.05	51.68	72.56	9.4186	6.8681	28.17
N17	50	1200	36	48.55	72.55	51.17	72.67	9.4186	6.8681	27.99

the RSM experimental design setting runs for two purposes: (i) to provide a measure of process stability and inherent variability and (ii) to check for curvature. In an unblocked RSM design, the number of centerpoints control other properties of the design matrix. The number of centerpoints can produce an orthogonal design or produce "uniform precision." Uniform precision ensures that the variance of prediction is the same at the center of the experimental space as it is at a unit distance away from the center.

Figure 1 illustrates an overview of the complete production process implemented, so as to obtain the HAp in powder form from its aqueous suspension form at the chemical precipitation stage. The factors and responses are presented for the stages of the process, in which they are controlled and evaluated, respectively. The factors which remained constant are also presented. These factors were considered to exert a lower level of significance over the effects of the responses studied, as identified at the screening stage of the investigation. The HAp powders in this study were synthesized based on the same chemical precipitation reaction used in Kehoe et al. (Ref 19).

Phase analysis of the HAp powder particles were performed on a Bruker Advance D8 XRD using Cu Kα radiation at 40 kV and 40 mA. The scanning range (2θ) was performed from 20° to 60° with a step size of 0.02°, at a scan speed of 2θ s^{-1}. XRD was used to evaluate the phases present (X_p) and determine crystallographic properties of the HAp powders to ensure compliance to regulatory requirements. Phase identification was performed with reference to the library database supplied by the International Centre for Diffraction Data (ICDD) by directly comparing the x-ray diffraction patterns to the Joint Committee for Powder Diffraction Standards (JCPDS) files for HAp (JCPDS, Card No. 9-432) and also the common phases present within calcium phosphate-based powders, such as, α-TCP (9-348), β-TCP (9-169), DCPA (9-80), DCPD (9-77), OCP (26-1056), TTCP (25-1137), and CHAp (19-272) in order to obtain an indication of the relative proportions of phases present in the powders analysed. The percentage crystallinity (X_c) was determined using the following equation (Ref 21, 22):

$$X_c\,(\%) = \frac{\sum A_C}{\sum A_C + \sum A_A} \times 100, \qquad \text{(Eq 3)}$$

where $\Sigma A_C + \Sigma A_A$ gave the sum of the area under all the HAp crystalline and amorphous peaks and ΣA_C yields the sum of the areas under the crystalline peaks present in the scan range between 20° to 60°. The x-ray diffraction data were used to assess crystallite size (L_{002} and L_{300}) based on

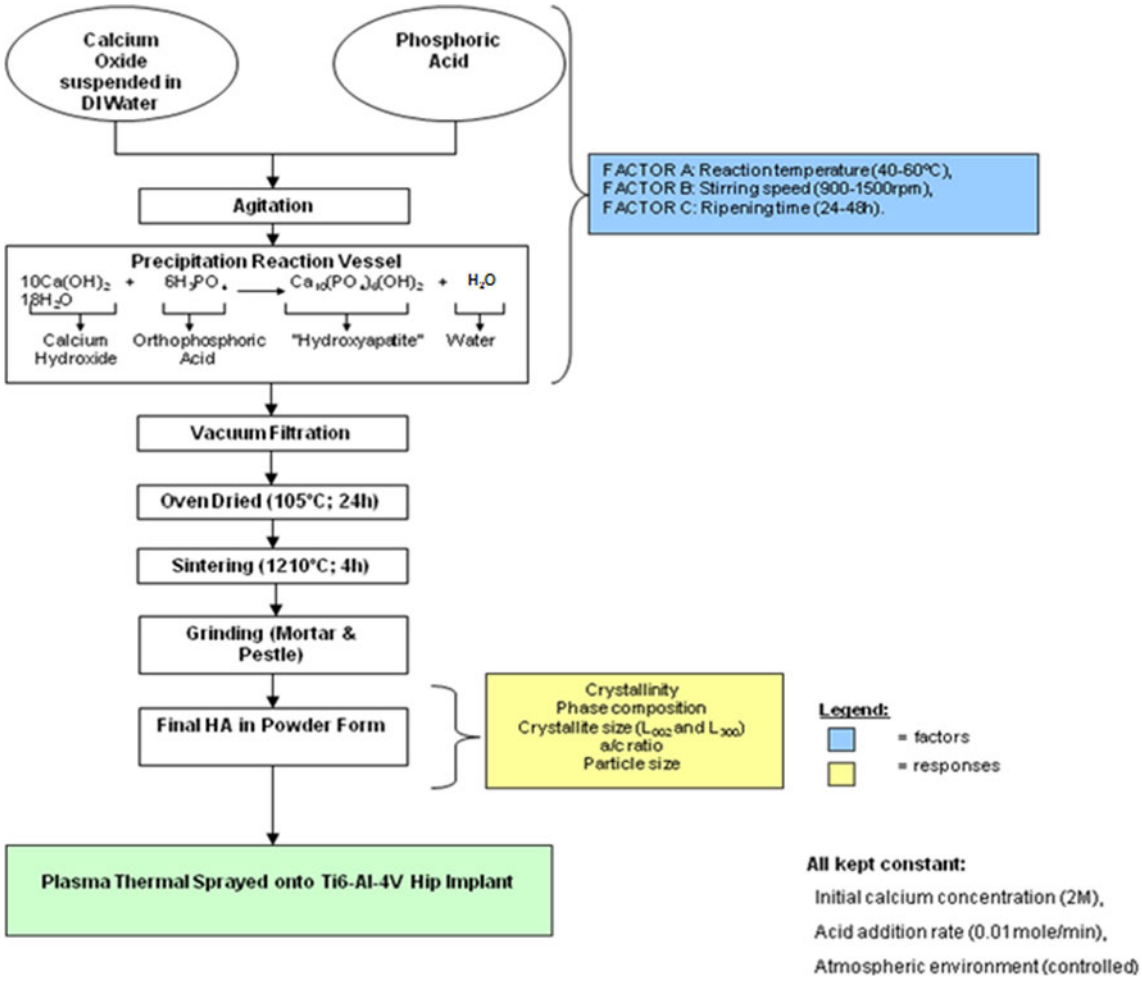

Fig. 1 Overview of the production process in obtaining HAp in powder form and the process variables and responses evaluated at the optimization Box-Behnken design stage

Scherrer's formula (see Eq. 4) from XRD peak broadness as follows (Ref 17, 21):

$$D = 0.9\alpha \text{ FWHM} \cos\theta, \quad \text{(Eq 4)}$$

where D is the crystallite size (nm), α the wavelength of monochromatic x-ray beam (0.15406 nm for Cu Kα) radiation. FWHM was the full width at half maximum of the diffraction peak under consideration (rad), and θ the diffraction angle (°). Lattice parameters, along the a and c axes were determined using unit cell refinement software package CelRef 3.0. Particle size (P_s) analysis was carried out with a Malvern Mastersizer to study the HAp powder particle sizes.

3. Experimental Results and Discussion

The results of the optimization stage of the three level Box-Behnken experimental design are presented in Table 1. Analysis of the regression coefficients of the linear polynomial models describing the relationship between the responses of phase purity (X_p), crystallinity (X_c), crystallite sizes (X_s, L_{002}, and L_{300}), lattice parameters (a and c), and mean particle size (P_s) against the three factors (T_o, V_{st}, t_r) are presented in the following sections. A comparison of the results obtained in this optimization investigation using Box-Behnken design is also compared against a previous screening study using fractional-factorial design (FFD) (Ref 19).

3.1 Phase Purity Model Development

As a result of analysing the measured responses using the Design Expert software, the fit summary selected the highest order polynomial where the additional terms are significant and the model was not aliased. Choosing the stepwise regression method led to the elimination of the insignificant model terms automatically. The ANOVA results for the phase purity showed a significant model, plus accounting for other adequacy measures like R^2 (0.9047), adjusted R^2 (0.8817), and predicted R^2 (0.8205), were shown to be high, thus the model was statistically significant and leaving out the calcium concentration did not significantly affect the results here as it did not have a major influence on the purity results in the screening study. A significant lack of fit can also be attributed to the elimination of the acid addition rate as a controlling factor. An adequate precision ratio of 21.046 indicated adequate model discrimination (Ref 23). The result of the ANOVA for the phase purity model showed that the main effect of two of the chemical precipitation parameters and the quadratic effect of the stirring speed were significant model terms. However, the reaction synthesis temperature was the factor which possesses the most significant main effect on the phase purity, with the stirring speed containing a lesser effect. However, the quadratic effect of the stirring speed was found to have a more significant effect, in comparison to being considered solely as a main effect. This result correlated well with literature, which suggests that both the temperature and stirring speed are critical in controlling the final phase purity (Ref 24). The order of significance for these effects follows the order: $T_o > V_{st}^2 > V_{st}$. The final model in terms of coded factors is presented in Eq 5.

$$\text{Phase purity, } X_p, (\%) = 45.13 - 16.06(T_o) + 8.83(V_{st}) + 20.61(V_{st})^2, \quad \text{(Eq 5)}$$

The above equation (5) indicates that the order of the level of significance of the positive effects of the chemical precipitation process parameters on the phase purity follows the order: $(V_{st})^2 > (V_{st})$ while the order of the level of significance of the negative effects on the lattice parameter ratio was T_o only.

The 3D surface and 2D contour plots illustrated in Fig. 2(a) and (b) examined the effect of the two significant factors (reaction temperature and stirring speed) on the phase purity response. The results indicate that both the reaction synthesis temperature and the stirring speed exert a significant effect on the response for phase purity. The positive response of the stirring speed indicates that higher levels of stirring speed are required, while the negative effect for the reaction synthesis temperature indicated that a lower temperature, in the range of about 40 °C is optimum for increased the responses of phase purity. This optimum temperature was in good agreement with Afshar et al. (Ref 14) and Saeri et al. (Ref 15). It was evident from Fig. 2 that in the case of the steep curvilinear effect representing the stirring speed, the response is highly sensitive to this factor, with a sharp increase in phase purity. While the steep slope in the case of the reaction synthesis temperature indicated that the response was relatively sensitive to this factor, with an increase of parameter resulting in a decrease of the phase purity obtainable.

Table 2 shows the top four most influencing main and interaction effects, in chronological order, for both the screening

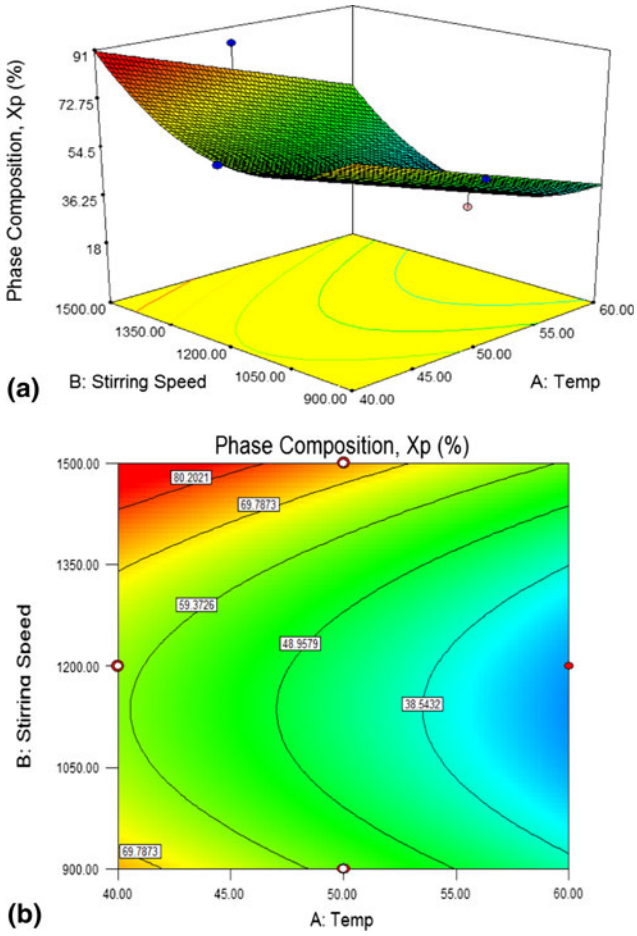

Fig. 2 3D surface (a) and contour plot (b) of phase purity at a ripening time of 48 h

Table 2 Comparison of significant effects for screening (Stage I) and optimization (Stage II) for phase purity, X_p

	↑Purity, X_p, %	
Order of significance	**Fractional-factorial design (FFD)**	**Box-Behnken design (BBD)**
1	↑V_{ac} * V_{st}	↑V_{st}^2
2	↑V_{ac} * T_o * atm.	↓T_o
3	↑t_r	↑V_{st}
4	↑T_o	

(FFD) (Ref 19) and optimization (BBD) with respect to attaining high levels of phase purity. First, interactions involving the acid addition rate and calcium concentration did not appear in the BBD, as it was excluded from this design. One main influencing factor that appeared in the screening but not in the optimization was the ripening time. Clearly, this has no significant effect on the ranges studied for the optimization (24-48 h) as opposed to the broader range (0.5-48) investigated during the screening stage.

3.2 Crystallinity Model Development

By selecting the stepwise regression method, the insignificant model terms were automatically eliminated. The resulting adequate precision ratio of 28.021, indicated adequate model discrimination was achieved and shows that elimination of the acid addition rate and the calcium concentration did not have an influence on attaining a significant model. The order of significance for these effects follows the order: $T_o^2 > t_r^2 > V_{st} > T_o > T_o * V_{st} > V_{st} * t_r > T_o * t_r > V_{st}^2$. The final model in terms of coded factors is shown below in Eq 6.

$$\begin{aligned}\text{Crystallinity}, X_c, (\%) = {} & 1.73(T_o) + 2.14(V_{st}) + 1.13(T_o * V_{st}) \\ & - 0.64(T_o * t_r) - 0.72(V_{st} * t_r) \\ & + 4.80(T_o^2) + 0.51(V_{st}^2) + 3.00(t_r^2)\end{aligned} \quad \text{(Eq 6)}$$

The above equation (6) indicates that the order of the level of significance of the positive effects of the chemical precipitation process parameters on the crystallinity follows the order: $(T_o^2) > (t_r^2) > (V_{st}) > (T_o) > (T_o * V_{st}) > (V_{st}^2)$ while the order of the level of significance of the negative effects on the lattice parameter ratio was as follows: $(V_{st} * t_r) > (T_o * t_r)$.

Figure 3(a) and (b) shows the 2D contour graphs, highlighting the significant interaction effect between the reaction temperatures and stirring speed at ripening times of between 24 and 48 h. It is clear from this figure that an increase in both factors resulted in a marked increase in crystallinity, while the ripening time has little effect between 24 and 48 h, demonstrating a difference in crystallinity of 2.71%. The maximum crystallinity of 86.96% occurs at a reaction synthesis temperature of 60 °C and a stirring speed of 1500 rpm at a ripening time of 24 h. The stirring speed has a slightly positive effect on the crystallinity (Fig. 3). In the case of the reaction temperature, the curvilinear effect demonstrates that increasing the temperature until it reaches its maximum value would result in enhanced crystallinity, with decreased levels obtained at approximately mid-range (50 °C). The nonsignificance of the ripening time was also demonstrated whereby there is little or no effect in varying the ripening time between 24 and 48 h,

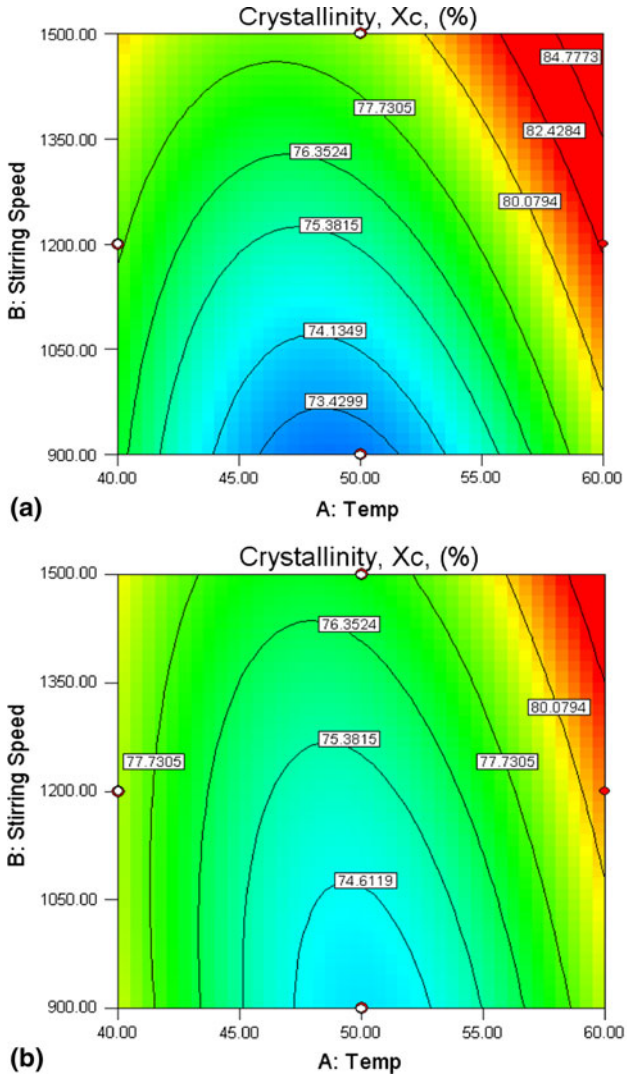

Fig. 3 2D contour plots of crystallinity at (a) a ripening time of 24 h and (b) a ripening time of 48 h

Table 3 Comparison of significant effects for screening (Stage I) and optimization (Stage II) for crystallinity, X_c

	↑Crystallinity, X_c, %	
Order of significance	**Fractional-factorial design (FFD)**	**Box-Behnken design (BBD)**
1	↑t_r	↑T_o^2
2	↑T_o * atm	↑t_r^2
3	↓atm	↑V_{st}
4	↑V_{ac} * Ca^{2+}	↑T_o

with the minimum crystallinity being obtained at 36 h. Increasing the stirring speed resulted in a direct increase of crystallinity.

Table 3 shows the top four most influencing main and interaction effects, in chronological order, for both the screening (FFD) and optimization (BBD) with respect to attaining high levels of crystallinity. Since the acid addition rate, calcium concentration and atmospheric control (as factors) were

eliminated from the optimization study; their effects do not appear as being significant in the BBD model developed for crystallinity. The reaction temperature and the ripening time effects appear in both models. However, their quadratic effects included on the BBD model, shows that their level of significance had increased dramatically within the ranges investigated. These factors were discussed, at the screening stage, in relation to their effects on crystallinity. Hence, these observations would also apply here. However, the stirring speed was now introduced as a significant main effect in the top four most influencing factors effecting crystallinity during optimization. Instead, the screening results showed the stirring speed to have a less significant effect on the crystallinity (Ref 19). Therefore, it had increased in level of significance due to the elimination of other factors (such as, acid addition rate, calcium concentration, and atmospheric control). It would be expected that the stirring speed would affect the crystallinity as higher mixing intensities were required to attain high levels of crystallinity (Ref 25).

3.3 Crystallite Size (L_{002} and L_{300}) Model Development

Choosing the stepwise regression method led to the elimination of insignificant model terms automatically. An adequate precision ratio of 6.1602 and 8.227 was found from the ANOVA results for both crystallite sizes (L_{002} and L_{300}), respectively, showing that adequate model discrimination has been achieved for both models (Ref 20, 23). The lack of fit in both cases was significant, with a transformation required in the case of the crystallite size in the 300 plane to improve model adequacy. Again, this may be attributed to eliminating the factors (acid addition rate, calcium concentration, and atmospheric control) included in the screening study, as it had either an interaction effect (V_{ac} * t_r) or a main effect and interaction effect (V_{ac} * atm) for the crystallite size, L_{002} and L_{300}, respectively (Ref 19). Therefore, eliminating the acid addition rate and atmospheric control appeared to affect the models produced here and produce a significant lack of fit. The result of the ANOVA for the crystallite size model, L_{002}, showed that while the main effect of the reaction temperature had a significant effect on the crystallite size in this plane, the quadratic effect of ripening time has a greater level of significance. The order of significance for these effects follows the order: $t_r^2 > T_o$. The ANOVA for the crystallite size model, L_{300}, shows instead, that the stirring speed (main and quadratic) was the most significant factor, while the quadratic effect of ripening time has a lesser significance on the final crystallite size for the 300 plane. The order of significance for these effects follows the order: $V_{st} > V_{st}^2 > t_r^2$.

The final mathematical models for the crystallite size responses, L_{002} and L_{300} in terms of coded factors as determined by the Design Expert software are shown in Eq 7 and 8.

$$\text{Crystallite size}, L_{002}, \text{nm} = 52.86 + 4.71(T_o) + 7.96(t_r)^2 \quad \text{(Eq 7)}$$

$$\text{Crystallite size}, L_{300}, \text{nm} = 71.86 + 8.28(T_o) - 8.63(T_o)^2 - 8.63(t_r)^2 \quad \text{(Eq 8)}$$

Equation (7) indicated that two effects were positively affecting the crystallite size (L_{002}) in the same order as shown previously: $t_r^2 > T_o$ while Eq 8 indicates that the only positive

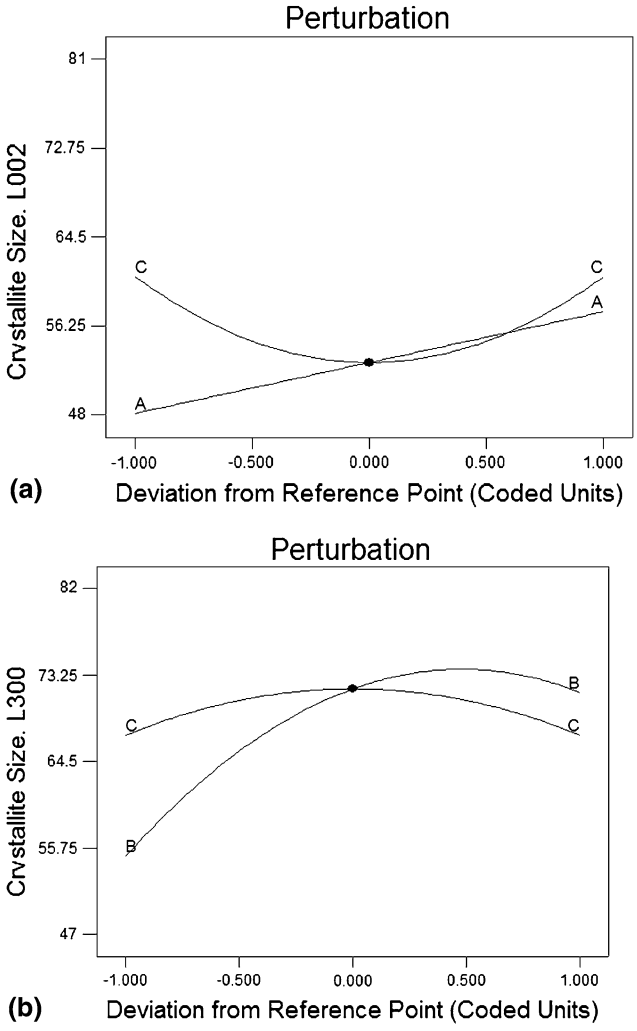

Fig. 4 Perturbation plot showing the effect of all the parameters on the crystallite size, L_{002} (a) and L_{300} (b)

effects of the chemical precipitation process parameters on the crystallite size (L_{300}) is (T_o) while the order of the level of significance of the negative effects on the lattice parameter ratio was as follows: $(T_o^2) > (t_r^2)$.

The perturbation plot aids in comparing the effect of the significant factors at a particular point in the design space. Figure 4(a) shows a comparison between the significant effects of reaction temperature and ripening time on the crystallite size, L_{002}, while Fig. 5(b) shows a comparison between the significant effects of stirring speed and ripening time on the crystallite size. In Fig. 4(a), it was evident that the positive linear relationship of the reaction temperature indicates that an increase in this parameter directly increased the crystallite size, while the curvilinear relationship of the ripening time shows that the L_{002} crystallite size was at its minimum mid-range (at 36 h). Figure 4(b) shows the comparison between the significant effects of both the stirring speed and ripening time, both of which exhibit curvilinear relationships with the crystallite size in the 300 plane. For this plane, an increase of stirring speed would result in an increase of the crystallite size, although the crystallite size was at its minimum at a ripening time of 36 h and highest values at 24 and 48 h ripening.

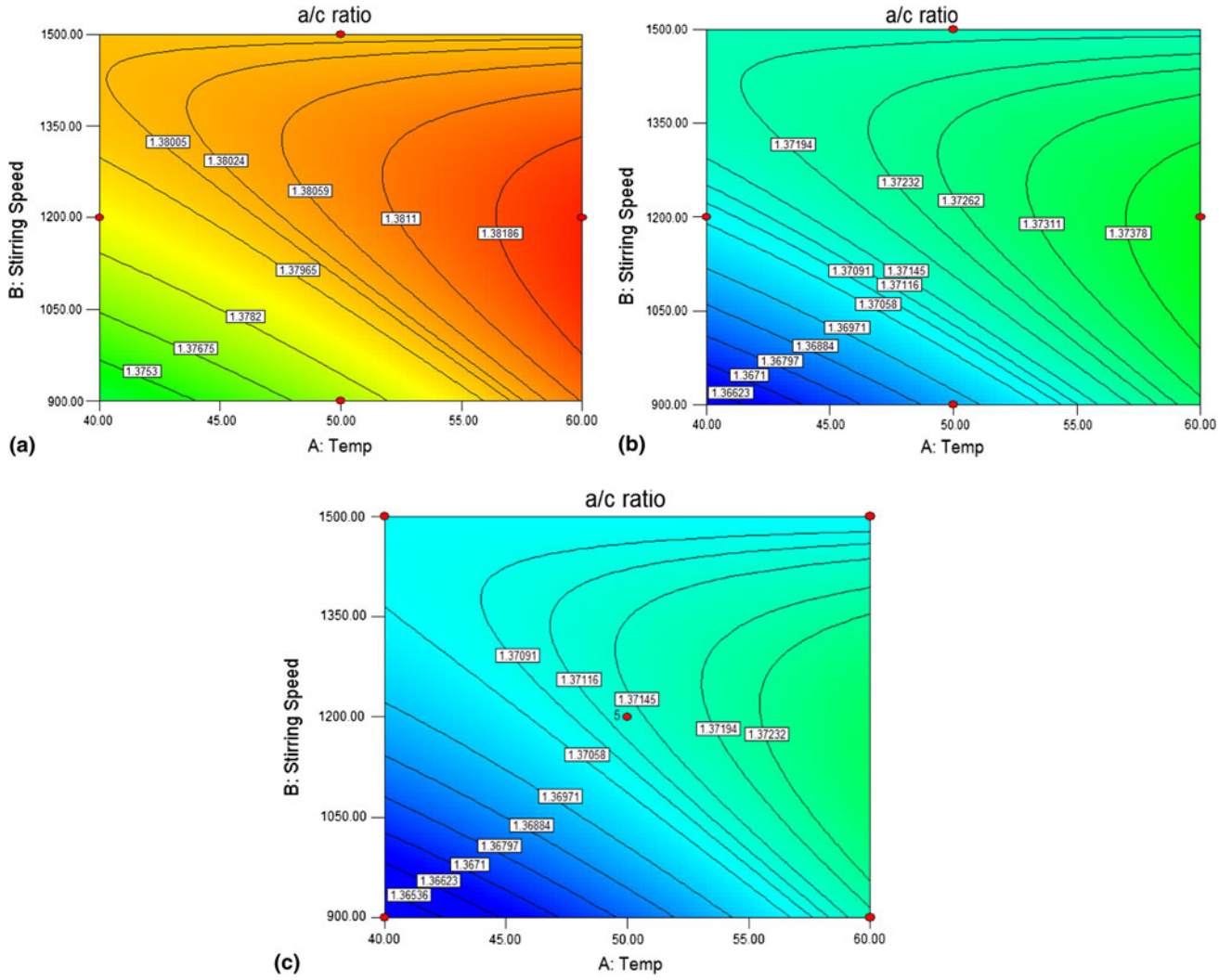

Fig. 5 2D contour plots of lattice parameter ratio at (a) a ripening time of 24 h; (b) a ripening time of 36 h, and (c) a ripening time of 48 h (under an inert environment)

Table 4 Comparison of significant effects for screening (Stage I) and optimization (Stage II) for crystallite size, L_{002}

	↑Crystallite size, L_{002}, nm	
Order of significance	**Fractional-factorial design (FFD)**	**Box-Behnken design (BBD)**
1	↑atm	↑T_o
2	↑T_o * t_r	↑t_r^2
3	↓Ca^{2+}	
4	↑V_{ac} * t_r	

Table 5 Comparison of significant effects for screening (Stage I) and optimization (Stage II) for crystallite size, L_{300}

	↓Crystallite size, L_{300}, nm	
Order of significance	**Fractional-factorial design (FFD)**	**Box-Behnken design (BBD)**
1	↑t_r	↑V_{st}
2	↑T_o * atm	↑V_{st}^2
3	↓atm	↑t_r^2
4	↑V_{ac} * Ca^{2+}	

Tables 4 and 5 shows the top four most influencing main and interaction effects, in chronological order, for both the screening (FFD) and optimization (BBD) with respect to attaining high levels of crystallite size in the 002 and 300 plane, respectively. For L_{002}, atmospheric control, calcium concentration, and acid addition rate were eliminated in the Box-Behnken design. Therefore, the remaining factors (T_o and t_r) that were originally found to affect this response have increased in their level of significance in attaining a high crystallite size. While for L_{300}, the same approach applied. However, the significance of the stirring speed was now included during optimization. This factor was previously ranked the fifth most influencing factor for this response. Therefore, it may be assumed that the removal of the other factors has resulted in this increase of significance. Clearly, it was noted that it has an influence similar to that for crystallinity. However, the stirring speed and reaction temperature did not appear to significantly affect the crystallite size for the 002 and 300 plane, respectively. The difference for these

models (screening and optimization) may be attributed to the variance in the range of factors selected.

3.4 Lattice Parameter Ratio Model Development

Choosing the stepwise regression method led to the automatic elimination of the insignificant model terms. An adequate precision ratio of 17.249 indicated adequate model discrimination (Ref 10). The predicted R^2 in this model was not as high as that obtained for the screening model, so therefore the elimination of the factors (acid addition rate, calcium concentration, and atmospheric) resulted in this decrease, since the interaction of the acid addition rate and calcium concentration was ranked as the fourth most significant effect in the screening model and moreover, either of the two factors were involved in interactions with other factors at ranks below this. The result of the ANOVA for the lattice parameter ratio model shows that the main effect of all three of the chemical precipitation parameters investigated have a significant effect on the lattice parameter ratio. An interaction effect between the reaction synthesis temperature and the stirring speed quadratic effect of the stirring speed are significant model terms, while the quadratic effects of both the stirring speed and ripening time are also shown to be influencing factors. The order of significance for these effects followed the order: $t_r > t_r^2 > T_o > V_{st}^2 > T_o * V_{st} > V_{st}$.

The final model in terms of coded factors is shown in Eq 9. This equation indicated that the order of the level of significance of the positive effects of the chemical precipitation process parameters on the lattice parameter ratio follows the order: $(t_r^2) > (T_o) > (V_{st})$ while the order of the level of significance of the negative effects on the lattice parameter ratio was as follows: $(t_r) > (V_{st}^2) > (T_o * V_{st})$.

$$a/c \text{ ratio} = 1.37 + 1.821\text{E} - 003(T_o) + 1.223E - 003(V_{st}) - 4.086E - 003(t_r) - 1.823E - 003(T_o * V_{st}) - 1.968E - 003(V_{st})^2 + 5.276E - 003(t_r)^2 \quad \text{(Eq 9)}$$

Equation 9 indicates that the order of the level of significance of the positive effects of the chemical precipitation process parameters on the lattice parameter ratio followed the order: $(t_r^2) > (T_o) > (V_{st})$ while the order of the level of significance of the negative effects on the lattice parameter ratio was as follows: $(t_r) > (V_{st}^2) > (T_o * V_{st})$.

Figure 5(a-c) shows the 2D contour graphs, highlighting the significant interaction effect between the reaction temperatures and stirring speed at ripening times of between 24 and 48 h. It was clear from this figure that an increase in the reaction temperature produced a marked increase in ratio, while a reduction in the ripening time appeared to favor this response. A median value (1200 rpm) of stirring speed also appeared to favor an increase in lattice parameter ratio. Figure 5 confirmed how a direct increase of the reaction temperature can increase the resulting a/c ratio, while a curvilinear relationship for the ripening time represents a high sensitivity of this factor to the a/c ratio, with decreased ripening times dramatically increasing this response. A less pronounced curvilinear effect for the stirring speed produced a maximum lattice ratio when 1200-1500 rpm was chosen.

Table 6 shows the top four most influencing main and interaction effects, in chronological order, for both the screening (FFD) and optimization (BBD) with respect to attaining lattice parameters within a desired range. With the exception of the calcium concentration, all the other factors (t_r, V_{st}, and T_o) were the same for both models, with the quadratic effects of certain factors included in the optimization model. The reasons for their influencing the lattice parameter ratio were valid for both models, as discussed previously (Ref 19).

Table 6 Comparison of significant effects for screening (Stage I) and optimization (Stage II) for the lattice parameter ratio, *a/c*

	↓Lattice parameter ratio, *a/c*	
Order of significance	**Fractional-factorial design (FFD)**	**Box-Behnken design (BBD)**
1	$\uparrow t_r$	$\downarrow t_r^2$
2	$\uparrow V_{st}$	$\uparrow t_r$
3	$\uparrow T_o$	$\uparrow V_{st}^2$
4	$\uparrow V_{ac} * Ca^{2+}$	$\uparrow T_o * V_{st}$

3.5 Particle Size Model Development

Choosing the stepwise regression method led to the automatic elimination of the insignificant model terms. The ANOVA results showed $R^2 = 0.6250$; predicted $R^2 = 0.3185$; adjusted $R^2 = 0.5385$, and an adequate precision = 7.330 indicated adequate model discrimination (Ref 23). However, factors (such as acid addition rate and calcium concentration) were found to be included as one of the top four most influencing factors having an effect on the particle size in the screening model are not accounted for in this model. The result of the ANOVA for the particle size model shows that the main effect of one (reaction synthesis temperature) of the chemical precipitation parameters investigated had a significant effect on the lattice parameter ratio. An interaction effect between the stirring speed and the ripening time and a quadratic effect of the ripening time were the significant model terms influencing final response for particle size. The order of significance for these effects followed the order: $t_r^2 > V_{st} * t_r > T_o$.

The final model in terms of coded factors is shown in Eq 10. The equation indicates that all of the significant effects are positively affecting the lattice parameter ratio in the same order as shown previously: $(t_r^2) > (V_{st} * t_r) > (T_o)$.

$$\text{Particle size, } P_s\,(\mu\text{m}) = 25.49 + 2.15(T_o) + 3.95(V_{st} * t_r) + 5.90(t_r)^2 \quad \text{(Eq 10)}$$

The perturbation plot shown in Fig. 6 shows a comparison between the effects of reaction temperature, stirring speed, and ripening time on the maximum particle size. This confirms how an increase in both the reaction temperature and the ripening time could significantly increase the resulting particle size, while a linear response for the stirring speed is shown to have little effect on tailoring the desired particle size. The curvilinear relationship of the ripening time demonstrates a high sensitivity for this factor to the final response with the minimum response for particle size found at 36 h and its maximum found at the lower (24 h) and upper (48 h) limits. The linear response for the reaction temperature indicated a less significant response. However, the plot also demonstrates how a direct increase in the reaction temperature can also maximize the final particle size.

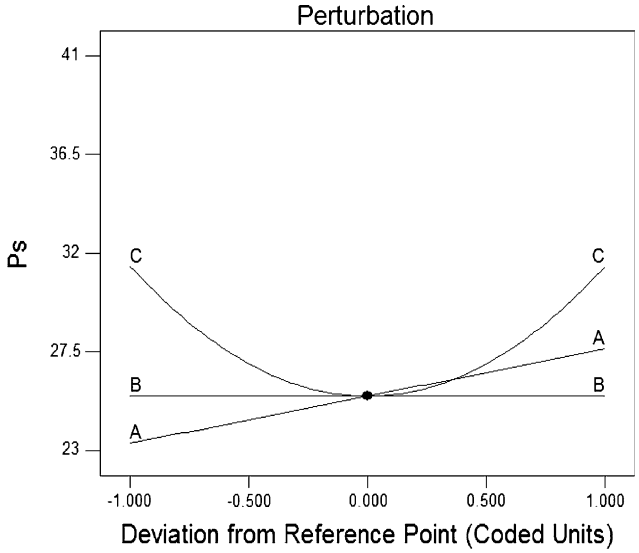

Fig. 6 Perturbation plot showing the effect of all the parameters on the particle

Table 7 Comparison of significant effects for screening (Stage I) and optimization (Stage II) for the particle size, P_s

	↓Particle size, P_s	
Order of significance	**Fractional-factorial design (FFD)**	**Box-Behnken design (BBD)**
1	↑T_o	↓t_r^2
2	↑Ca^{2+}	↓V_{st} * t_r
3	↓V_{ac} * T_o	↓T_o
4	↑V_{ac} * Ca^{2+}	

Table 7 shows the top four most influencing main and interaction effects, in chronological order, for both the screening (FFD) and optimization (BBD) with respect to attaining particle sizes with the desired range. Comparing the top four most influencing effects in both models, it was obvious that the reaction temperature, as expected, had a major influence over the resulting particle size. However, the influence of this factor appears to have the opposite effect: requiring an increase in the screening model and a decrease in the optimization model to effectively increase the particle size. This may be explained by the fact that the temperature range varied between the models developed (that is, 20-60 °C for screening (Ref 19) and 40-60 °C for optimization). As a result it may be interpreted that, while an increase in the reaction temperature is known to result in an increase in particle size, the optimum temperature for acquiring the largest particle size may in fact lie around 40-50 °C. The desirability approach (used at a later stage), however, also indicates that use of a high reaction temperature was required to increase the particle size.

3.6 Desirability Approach

The RSM study has aided in the development of six response models, relating the phase purity, crystallinity, crystallite sizes (L_{002} and L_{300}), lattice parameter ratio and particle size to the three factors investigated. However, the DoE in this investigation excluded any experiment being conducted, which examined the effect of setting all three factors at the upper level, and for this reason the models developed in the fractional-factorial design study (screening) were instead used to identify the most appropriate combination of factors in order to achieve the optimum response, with respect to the HAp powder characteristics studied. These models also incorporated the full list of chemical precipitation parameters (acid addition rate, reaction temperature, stirring speed, ripening time, initial calcium concentration, and atmospheric control) of which have been shown in literature to determine the final powder characteristics. Design Expert has the capability in generating numerous possible solutions based on the optimization criteria selected. The desirability (0-1) of each solution is indicated. The optimum solutions for the fractional-factorial and Box-Behnken models are shown in Table 8. The preferred settings can then be selected manually. The importance level for each response within this desired optimization analysis was selected. The phase purity and crystallinity were set to an importance level of 5. The lattice parameter ratio was set to an importance level of 3, while the particle size and crystallite sizes in the 002 and 300 plane were set to an importance level of 2. The goal and importance for each optimization parameter used is shown in Table 9. Design Expert has the capability in generating numerous possible solutions based on the optimization criteria selected. The desirability (0-1) of each solution can be determined.

Table 8 Perturbation plot showing the effect of all the parameters on the HAp powder characteristics

	Optimized solutions		Experimental values	FDA
	BBD	**FFD**	**N16**	**Req.**
Factor				
Acid addition rate, mol/min	0.01	0.01	0.01	
Reaction temperature, °C	40	60	60	
Stirring speed, rpm	900	1500	1500	
Ripening time, h	48	48	48	
Calcium concentration, *M*	2.0	2.0	2.0	
Atmospheric control, yes/no	Yes	No	No	
Response				
Phase purity, %	72.9638	97.5919	98.8886	>95
Crystallinity, %	79.2267	91.2467	95.1881	>95
Crystallite size, L_{002}, nm	56.1037	102.0189	107.9240	
Crystallite size, L_{300}, nm	50.2599	85.6456	90.5307	
Lattice parameter ratio, *a*/*c*	1.3658	1.3692	1.3692	
Particle size, μm	25.2888	19.2181	15.3800	<100
Desirability	**0.695**	**0.447**		

The results in Table 8 are compared against actual experimental results obtained at the same experimental conditions (that is, N16, however, from the fractional-factorial (screening) model; Ref 19). The fractional-factorial solution shows that the

model is predicting each response to be smaller in comparison to those obtained experimentally at the same conditions (N16). This can be attributed to the fact that the model is predicting the responses through incorporating the full set of models obtained, while the experimental conditions represent a true indication of the real values which can be obtained at the same conditions (factors). However, the model and the experimental conditions succeeded in verifying that the same set of factors were required in order to tailor the desired powder characteristics to meet with minimum regulatory requirements. The Box-Behnken design, however, provides a set of factors which do not match that of the N16 experimental set-up. Although it shows a high desirability of 0.695 (in comparison to 0.447 for the fractional-factorial design), the main regulatory requirements for minimum phase purity and crystallinity was not attained. Therefore, the effect of leaving out the acid addition rate, calcium concentration, and atmospheric control is found to exert a major effect on producing a HAp powder satisfying the minimum regulatory requirements. Thus, researchers (Ref 18) cannot accurately optimize the desired HAp powder characteristics, while eliminating any of the influences for all of the precipitation process parameters as proved by Table 8. The other factors (acid addition rate, calcium concentration, and atmospheric control) must also be included.

A desirability bar graph for each response in both the Fractional-Factorial and Box-Behnken design is shown in Fig. 7. The bar charts show that less important responses (requiring control for regulatory purposes) received a high desirability rating than the more critical responses (such as, phase purity and crystallinity). However, in terms of actual, predicted, and experimental results (N16), the overall realistic outcome benefits what was desired. Therefore, Fig. 7 further confirms that all of the process factors studied (three or more) need to be set as high as possible in order to obtain the desired responses for a phase pure and highly crystalline HAp, of particle size not exceeding 100 μm.

Table 9 Design optimization parameters

	Goal	Importance
Phase purity, %	Maximize	+++++
Crystallinity, %	Maximize	+++++
Crystallite size, L_{002}, nm	Maximize	++
Crystallite size, L_{300}, nm	Minimize	++
Lattice parameter ratio, a/c	Minimize	+++
Particle size, μm	In range	++

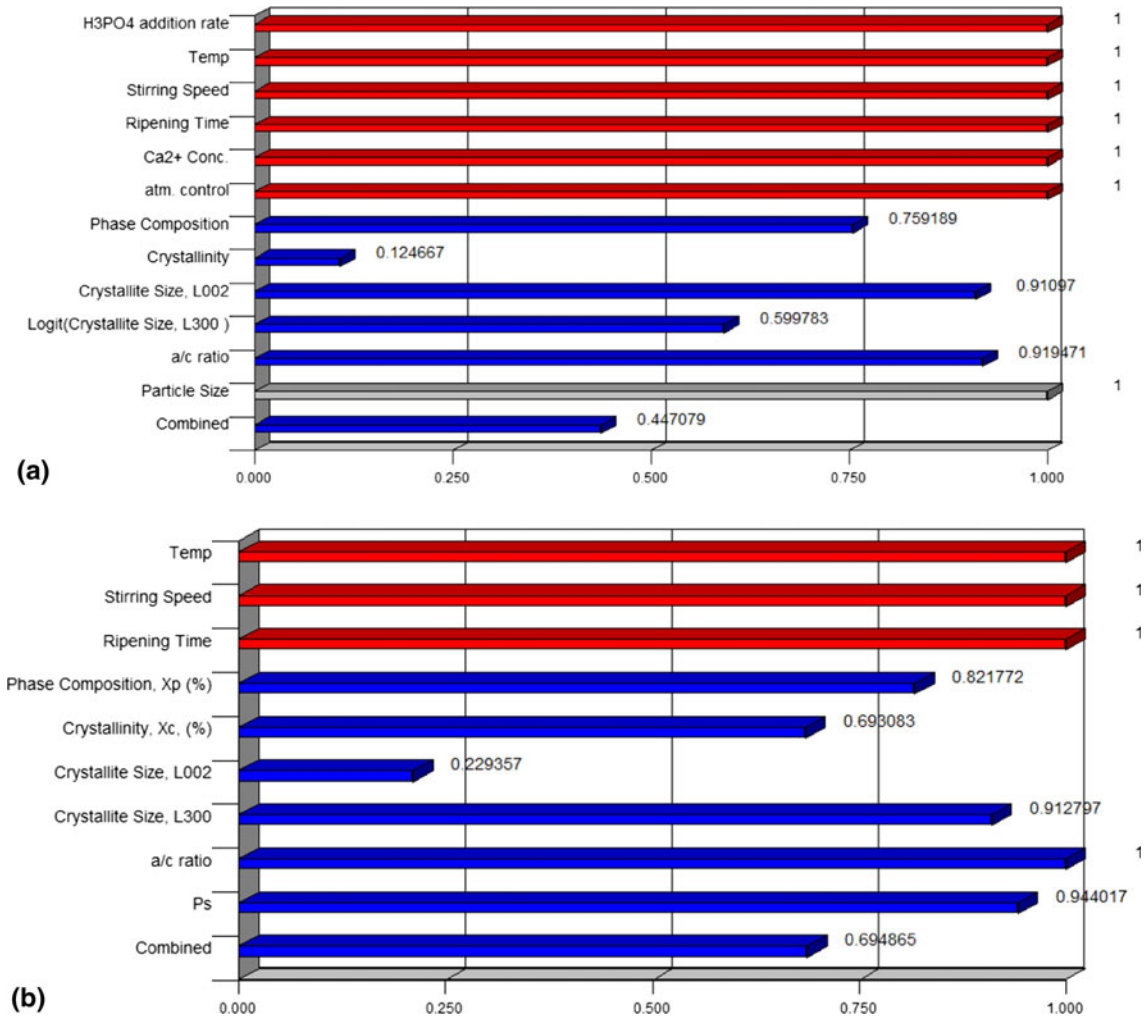

Fig. 7 Desirability bar graph obtained for (a) the fractional-factorial model and (b) the Box-Behnken model

4. Conclusion

The Box-Behnken experimental design was applied to study a large number of variables in synthesis of HAp by the chemical precipitation method, and to analyze their influence on HAp properties. HAp possessing optimum powder characteristics for orthopedic application via a thermal spray technique can therefore be prepared using the following chemical precipitation process parameters: Reaction temperature 60 °C, ripening time 48 h, and stirring speed 1500 rpm using high reagent concentrations. Ripening time and stirring speed significantly affected the final phase purity for the experimental conditions of the Box-Behnken design. An increase in both the ripening time (36-48 h) and stirring speed (1200-1500 rpm) was found to result in an increase of phase purity from 47(±2)% to 85(±2)%. Crystallinity, crystallite size, lattice parameters, and mean particle size were also optimized within the research to find desired settings to achieve results suitable for FDA regulations.

Acknowledgment

This work is supported under the EMBARK Initiative Scheme by the Irish Research Council for Science and Engineering (IRCSET).

References

1. M. Vallet-Regi, Ceramics for Medical Applications, *R. Soc. Chem. Dalton Trans.*, 2001, **2**, p 97–108
2. S.W.K. Kweh, K.A. Khor, and P. Cheang, The Production and Characterization of Hydroxyapatite (HA) Powders, *J. Mater. Process. Technol.*, 1999, **89–90**, p 373–377
3. V.P. Orlovskii, V.S. Komlev, and S.M. Barinov, Hydroxyapatite and Hydroxyapatite-Based Ceramics, *Inorg. Mater.*, 2002, **38**, p 973–984
4. R.A. Young and D.W. Holcomb, Variability of Hydroxyapatite Preparations, *Calcif. Tissue Int.*, 1982, **34**, p 17–32
5. F. Fazan, "In Vitro Behaviour of Plasma Sprayed Hydroxyapatite Coatings," Ph.D. Thesis, University of Birmingham, Birmingham, 2000
6. V. Deram, C. Minichiello, R.N. Vannier, A. Le Maguer, L. Pawlowski, and D. Murano, Microstructural Characterizations of Plasma Sprayed Hydroxyapatite Coatings, *Surf. Coat. Technol.*, 2003, **166**, p 153–159
7. A.D. Papargyris, A.I. Botis, and S. Papargyri, Synthetic Routes for Hydroxyapatite Powder Production, *Key Eng. Mater.*, 2002, **206–213**, p 83–86
8. J.L. Xu, K.A. Khor, Z.L. Dong, Y.W. Gu, R. Kumar, and P. Cheang, Preparation and Characterization of Nano-Sized Hydroxyapatite Powders Produced in a Radio Frequency (rf) Thermal Plasma, *Mater. Sci. Eng. A*, 2004, **374**, p 101–108
9. R. Kumar, P. Cheang, and K.A. Khor, RF Plasma Processing of Ultra-Fine Hydroxyaptite Powders, *Mater. Process. Technol.*, 2001, **113**, p 456–462
10. FDA, *Calcium Phosphate (Ca-P) Coating Draft Guidance for Preparation of FDA Submissions for Orthopedic and Dental Endosseous Implants*, Food and Drug Administration, Washington, DC, 1992, p 1–14
11. "Standard Specification for Calcium Phosphate Coatings for Implantable Materials," ASTM F1609, American Society for Testing and Materials, 2003
12. "Implants for Surgery: Hydroxyapatite—Part 1: Ceramic Hydroxyapatite," ISO 13779-1, International Standards Organisation, 2000
13. "Standard Specification for Composition of Hydroxylapatite for Surgical Implants," ASTM F1185, American Society for Testing and Materials, 2003
14. A. Afshar, M. Ghorbani, N. Ehsani, M.R. Saeri, and C.C. Sorrell, Some Important Factors in the Wet Precipitation Process of Hydroxyapatite, *Mater. Des.*, 2003, **57**, p 197–202
15. M.R. Saeri, A. Afshar, M. Ghorbani, N. Ehsani, and C.C. Sorrell, The Wet Precipitation Process of Hydroxyapatite, *Mater. Lett.*, 2003, **57**, p 4064–4069
16. J.F. Conn and L.A. Jessen, Process for Producing Hydroxyapatite, U.S. Patent 4,324,772, 1982
17. I. Smiciklas, A. Onjia, and S. Raicevic, Experimental Design Approach in the Synthesis of Hydroxyapatite by Neutralization Method, *Sep. Purif. Technol.*, 2005, **44**, p 97–102
18. S. Lazic, S. Zec, N. Miljevic, and S. Milonjic, The Effect of Temperature on the Properties of Hydroxyapatite Precipitated from Calcium Hydroxide and Phosphoric Acid, *Thermochim. Acta*, 2001, **374**, p 13–22
19. S. Kehoe and J. Stokes, Design of Experiments Study of Hydroxyapatite Synthesis for Orthopaedic Application Using Fractional Factorial Design, *J. Mater. Eng. Perform.*, under review
20. S. Chatterjee and B. Price, *Regression Analysis by Example*, 2nd ed., Wiley and Sons Inc, New York, 1977, p 200–202
21. S. Koutsoploulos, Synthesis and Characterization of Hydroxyapatite Crystals: A Review Study on the Analytical Methods, *J. Biomed. Mater. Res.*, 2002, **15**, p 600–612
22. K. Rogers, The Use of Diffraction for the Analysis of Biomaterials, *2nd Annual Biomaterials Workshop*, Cranfield University, UK, 2004
23. D. Rocak, M. Kosec, and A. Degen, Ceramic Suspension Optimization Using Factorial Design of Experiments, *J. Eur. Ceram. Soc.*, 2002, **22**, p 391–395
24. C. Kothapalli, M. Wei, A. Vasiliev, and M. Shaw, Influence of Temperature and Concentration on the Sintering Behaviour and Mechanical Properties of Hydroxyapatite, *Acta Mater.*, 2004, **52**, p 5655–5663
25. M. Giulietti, M.M. Seckler, S. Derenzo, M.I. Re, and E. Cekinski, Industrial Crystallisation and Precipitation from Solutions: State of the Technique, *Brazil. J. Chem. Eng.*, 2001, **15**, p 423–440